CBP-872/LBNL-xxxx (Mar. 25, 2011)

Electron-Cloud Build-Up: Theory and Data*

M. A. Furman,† Center for Beam Physics, LBNL, Berkeley, CA 94720,
and CLASSE, Cornell University, Ithaca, NY 14853

Abstract

We present a broad-brush survey of the phenomenology, history and importance of the electron-cloud effect (ECE). We briefly discuss the simulation techniques used to quantify the electron-cloud (EC) dynamics. Finally, we present in more detail an effective theory to describe the EC density build-up in terms of a few effective parameters.

For further details, the reader is encouraged to refer to the proceedings of many prior workshops, either dedicated to EC or with significant EC contents, including the entire "ECLOUD" series [1–22]. In addition, the proceedings of the various flavors of Particle Accelerator Conferences [23] contain a large number of EC-related publications. The ICFA Beam Dynamics Newsletter series [24] contains one dedicated issue, and several occasional articles, on EC. An extensive reference database is the LHC website on EC [25].

THE BASIC OVERALL PICTURE

The qualitative picture of the development of an electron cloud for a bunched beam is as follows:

1. Upon being injected into an empty chamber, a beam generates electrons by one or more mechanisms, usually referred to as "primary," or "seed," electrons.

2. These primary electrons get rattled around the chamber from the passage of successive bunches.

3. As these electrons hit the chamber surface they yield secondary electrons, which are, in turn, added to the existing electron population.

This process repeats with the passage of successive bunches. The EC density n_e grows until a saturation level is reached. The density gradually decays following beam extraction, or during the passage of a gap in the beam. In many cases of interest, the net electron motion in the longitudinal direction, i.e. along the beam direction, is not significant, hence the electron cloud is sensibly localized. For this reason, in first approximation, it makes sense to study it at various locations around the ring independently of the others. In addition, given that the essential dynamics of the electrons is in the transverse plane, i.e. perpendicular to the beam direction, two-dimensional simulations are also a good first approximation to describe the build-up and decay. In some cases, such as the PSR, electron generation, trapping and ejection from quadrupole magnets is now known to be significant, and these electrons act as seeds for the EC buildup in nearby drift regions [26].

The main sources of primary electrons are: photoemission from synchrotron-radiated photons striking the chamber walls; ionization of residual gas; and electron generation from stray beam particles striking the walls of the chamber. Depending on the type of machine, one of these three processes is typically dominant. For example, in positron or electron storage rings, upon traversing the bending magnets, the beam usually emits copious synchrotron radiation with a $\sim$keV critical energy, yielding photoelectrons upon striking the vacuum chamber. In proton rings, the process is typically initiated by ionization of residual gas, or from electron generation when stray beam particles strike the chamber.

The above-mentioned primary mechanisms are usually insufficient to lead to a significant EC density. However, the average electron-wall impact energy is typically $\sim$100–200 eV, at which secondary electron emission is significant. As implied by the above description, secondary emission readily exponentiates in time, which can lead to a large amplification factor, typically a few orders of magnitude, over the primary electron density, and to strong temporal and spatial fluctuations in the electron distribution [27]. This compounding effect of secondary emission is usually the main determinant of the strength of the ECEs, and is particularly strong in positively-charged bunched beams (in negatively-charged beams, the electrons born at the walls are pushed back into the wall with relatively low energy, typically resulting in relatively inefficient secondary emission).

The ECE combines many parameters of a storage ring such as bunch intensity, size and spacing, beam energy [28], vacuum chamber geometry, vacuum pressure, and electronic properties of the chamber surface material such as photon reflectivity R_γ, effective photoelectric yield (or quantum efficiency) $Y_{\rm eff}$, secondary electron yield (SEY), characterized by the function $\delta(E)$ (E =electron-wall impact energy), secondary emission spectrum [29, 30], etc. The function $\delta(E)$ has a peak $\delta_{\max}$ typically ranging in $1-4$ at an energy $E = E_{\max}$ typically ranging in $200-400$ eV.

A convenient phenomenological parameter is the effective SEY, $\delta_{\rm eff}$, defined to be the average of $\delta(E)$ over all electron-wall collisions during a relevant time window. Unfortunately, there is no simple a-priori way to determine

*Work supported by the US DOE under contract DE-AC02-05CH11231 and by the CesrTA program. Invited talk presented at the ECLOUD10 Workshop (Cornell University, Oct. 8-12, 2010).

† mafurman@lbl.gov

$\delta_{\rm eff}$, because it depends in a complicated way on a combination of many of the above-mentioned beam and chamber parameters. If $\delta_{\rm eff} < 1$, the chamber walls act as net absorbers of electrons and n_e grows linearly in time following beam injection into an empty chamber. The growth saturates when the net number of electrons generated by primary mechanisms balances the net number of electrons absorbed by the walls. If $\delta_{\rm eff} > 1$, the EC grows exponentially. This exponential growth slows down as the space-charge fields from the electrons effectively neutralize the beam field, reducing the electron acceleration. Ultimately, the process stops when the EC space-charge fields are strong enough to repel the electrons back to the walls of the chamber upon being born, at which point $\delta_{\rm eff}$ becomes $= 1$. At this point, the EC distribution reaches a dynamical equilibrium characterized by rapid temporal and spatial fluctuations, determined by the bunch size and other variables. For typical present-day storage rings, whether using positron or proton beams, the spatio-temporal average n_e reaches a level $\sim 10^{10-12}$ m^{-3}, the energy spectrum of the electrons typically peaks at an energy below ~ 100 eV, and has a high-energy tail reaching out to keV's. Figure 1 illustrates the build-up of the electron cloud in the LHC.

If there is a gap in the beam, or if the beam is extracted, the cloud dissipates with a falltime that is controlled by the low-energy value of $\delta(E)$ [31]. In general, there is no simple, direct correlation between the risetime and the falltime.

In regions of the storage ring with an external magnetic field, such as dipole bending magnets, quadrupoles, etc., the EC distribution develops characteristic geometrical patterns. For typical fields in the range $B = 0.01 - 5$ T and typical EC energies < 100 eV, the electrons move in tightly-wound spiral trajectories about the field lines. In practice, in a bending dipole, the electrons are free to move in the vertical (y) direction, but are essentially frozen in the horizontal (x). As a result, the y-kick imparted by the beam on a given electron has an x dependence that is remembered by the electron for many bunch passages. It often happens that the electron-wall impact energy equals $E_{\rm max}$ at an x-location less than the horizontal chamber radius. At this location $\delta(E) = \delta_{\rm max}$, hence n_e is maximum, leading to characteristic high-density vertical stripes symmetrically located about $x = 0$ [32]. For quadrupole magnets, the EC distribution develops a characteristic four-fold pattern, with characteristic four-fold stripes [33].

In summary, the electron-cloud formation and dissipation:

- Is characterized by rich physics, involving many ingredients pertaining to the beam and its environment.
- Involves a broad range of energy and time scales.
- Is always undesirable in particle accelerators.
- Is often a performance-limiting problem, especially in present and future high-intensity storage rings.
- Is challenging to accurately quantify, predict and extrapolate.

The main goals of current research in electron-cloud physics are, in no particular order of importance or relevance:

- Identify the relevant variables in each case.
- Estimate the electron density, time dependence, incident flux at the walls of the chamber walls, etc.
- Compare predictions against measurements as thoroughly as possible; iterate the process and pin down the values of the relevant variables.
- Predict the magnitude of the effect in other cases; if possible, minimize the effect at the design stages of new machines.
- Define a relatively simple set of rules of thumb, or a simple effective theory, to approximately determine the severity of the effect.
- Design and implement mitigation or suppression mechanisms.

These latter mechanisms can be classified into passive and active. Passive mechanisms that have been employed at various machines include:

- Coating the chamber with low-emission substances such as TiN [34, 35], TiZrV [19, 36–42] and amorphous carbon (a-C) [43, 44].
- Etching grooves on the chamber surface in order to make it effectively rougher, thereby decreasing the effective quantum efficiency via transverse grooves [45] or the effective SEY via longitudinal grooves [46, 47].
- Implementing weak solenoidal fields ($\sim$10–20 G) to trap the electrons close to the chamber walls, thus minimizing their detrimental effects on the beam [48, 49]

In terms of active mechanisms, clearing electrodes [50, 51] show significant promise in controlling the electron cloud development. If an electron cloud is unavoidable and problematic, active mechanisms that have been employed to control the stability of the beam include tailoring the bunch fill pattern [52] and increasing the storage ring chromaticity [27]. Fast, single-bunch, feedback systems are under active investigation as an effective mechanism to stabilize electron-cloud induced coherent instabilities [53, 54].

BRIEF HISTORY: BCE AND CE

The year 1995 is a dividing mark in the history of the ECE. That year, a report was published describing a fast and peculiar transverse coupled-bunch instability at the Photon Factory (PF) at KEK [55] that arose only when the machine was operated with a positron beam. Unlike the

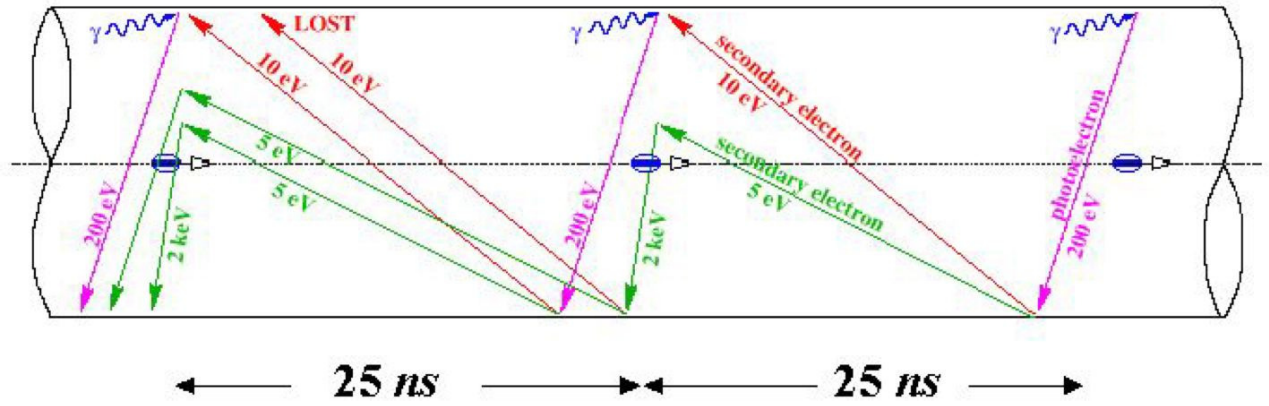

Figure 1: Cartoon illustrating the build-up of the electron cloud in the LHC for the case of 25-ns bunch spacing. The process starts with photoelectrons and is amplified by the secondary emission process. This cartoon was generated by F. Ruggiero.

ion-induced instability observed when the PF was operated with an electron beam, the positron beam instability persisted even with a substantial gap in the bunch train. The observed coupled-bunch mode spectrum for the positron beam was qualitatively different from that for an electron beam under otherwise similar conditions. The phenomenon disappeared when the bunch spacing was sufficiently large, and it could not be attributed to known machine impedances. The amplitude of the unstable motion reached saturation and was accompanied by the excitation of vertical coupled-bunch oscillations, and possibly of vertical emittance growth.

Experimental analysis [55], simulations [56] and analytical work [57] showed that the cause of the instability is an electron cloud (EC) that developed inside the vacuum chamber generated by photoelectron emission by synchrotron radiation from the beam striking the walls of the chamber. This photoelectron instability (PEI) [56] is one of many ECEs investigated in positron storage rings since then. The phenomenon was subsequently studied in dedicated experiments at BEPC [58] and the APS [59]. The ECE led to serious performance limitations at PEP-II and KEKB [60]. A closely related coupled-bunch instability was previously observed at CESR, although in this case the photoelectrons were trapped and localized in a section of the ring rather than spread out over most of the circumference [61]. A comprehensive program dedicated to measurements and analysis of ECE's for e^+e^- storage rings is now ongoing at CESR [62].

The above-mentioned ECE's are related to previously observed electron-proton dynamical effects such as beam-induced multipacting (BIM), first observed at the CERN proton storage ring ISR [63] when operated with bunched beams. Closely related to BIM is trailing-edge multipacting observed at the LANL spallation neutron source PSR [64], where electron detectors register a large signal during the passage of the tail of the bunch even for stable beams. All ECEs in e^+e^- as well as in hadron storage rings have precursors in the e-p instabilities for bunched and unbunched beams first seen at BINP in the mid-60s [65].

For the above reasons, 1995 marks the beginning[1] of the Common Era (CE) of the ECE (i.e., common to lepton and hadron rings). Before the Common Era (BCE), the only beam dynamics phenomena that were understood to be caused by electrons pertained to proton beams. As far as I know, 1997 was the first year in which ECEs from both positron and proton storage rings were discussed at the same meeting [2, 3].

OTHER CONSEQUENCES

Based on prior experience at the ISR, concerns arose in 1995-96 that electrons might spoil the LHC vacuum [66]. Early 1997 calculations showed that the LHC will be subject to an ECE [67], chiefly because the beam emits copious synchrotron radiation upon traversing the dipole bending magnets, with a critical photon energy

$$\frac{3\hbar c}{2\rho}\gamma^3 \simeq 44 \text{ eV} \tag{1}$$

where $\rho \simeq 2804$ m is the bending radius of the dipole magnets and $\gamma \simeq 7460$ is the usual relativistic factor of the proton beam at 7 TeV beam energy. The number of photons of all energies emitted per proton traversal through one bending magnet is given by

$$\frac{5\alpha\gamma}{2\sqrt{3}}\Delta\theta \simeq 0.4 \tag{2}$$

where $\alpha \simeq 1/137$ is the fine structure constant and $\Delta\theta \simeq 5$ mrad is the orbit bending angle through a single dipole. Roughly 50% of these photons have energies above the work function of the metal, leading to a substantial number of photoelectrons; as a result, the mechanism for the formation of the electron cloud in the LHC is analogous

[1] We choose the dividing line to be the publication year, 1995, even though the PF instability had been under study well before publication.

to present-day positron rings. Further calculations [67, 68], including the effects of secondary electron emission, quickly revealed the possibility of a substantial ECE. In this case, the primary concern was the power deposited by the electrons on the beam screen as they rattle around the chamber, which must be dissipated by the cryogenic system if the LHC superconducting magnets are to work as specified at nominal beam current. Since the cryogenic system was designed before the discovery of the ECE's in the LHC, substantial effort has been devoted since 1997 to better estimate the power deposition, to identify the conditions under which the cooling capacity may be exceeded, and to devise mitigation mechanisms if necessary. As part of this effort, the ECE has been experimentally studied at the SPS and the PS at the high beam intensities required for nominal LHC operation [25]. Recent experience at the LHC confirms the expectation of a significant ECE, even though the beam energy is presently only 3.5 TeV [69].

Another possible consequence of the EC is a strong increase in the vacuum pressure, produced by gas desorption by the electrons striking the walls. The phenomenon is strongly dependent on bunch current. The pressure rise exhibits a threshold behavior in beam current, and is sensitive to the bunch fill pattern at fixed total current, as observed in the B factories and the SPS [70]. When RHIC was operated with ion beams, the pressure rise was rather dramatic at transition energy due to the short bunch length, often triggering a beam abort by the machine protection system. By now this problem, related to the above-mentioned BIM at the ISR [63], has been controlled via low-emission coatings [36].

EC-induced single-bunch head-tail instabilities [71–73] have been predicted and observed at several storage rings. Before EC mitigation mechanisms were implemented at KEKB, such instabilities led to an effective beam blowup, becoming the most serious luminosity performance limitation. Bunch-to-bunch tune shift that grows towards the tail of the bunch train, sometimes leading to coupled-bunch instabilities, have also been observed [55, 74, 75].

Electrons from the cloud getting "sucked into" the body of a passing bunch typically lead to a rather significant head-tail tune spread. When this tune spread is combined with synchrotron oscillation and/or space-charge forces, incoherent effects result, such as slow emittance growth and/or particle losses. The bunch current threshold for such effects can be lower than for the above-mentioned single-bunch instabilities [53, 76–78].

A high-current instability that has been observed for many years at the PSR is also an ECE [64]. The phenomenon has been studied in intense, long-pulse, heavy-ion fusion drivers [79], at the J-PARC proton rings [80], and at the FNAL Main Injector [81, 82].

In summary:

- The ECE has been observed at many recent machines such as PF, PEP-II, KEKB, BEPC, PS, SPS, APS, RHIC, Tevatron, MI, SNS, CESRTA, DAΦNE and most recently the LHC, either through diminished performance or dedicated experiments.

- At the B factories PEP-II and KEKB, controlling the EC was essential to achieve and then exceed the luminosity goals. At PEP-II, an antechamber was incorporated into the design, designed to allow $\sim$99% of the photons to escape the chamber. In addition, the arc chambers were coated with TiN to reduce the SEY [34]. Elaborate fill patterns, designed to clear the electrons, were used for a while [52]. An effective suppression mechanism, implemented in both factories, was the installation of solenoidal magnetic fields to trap electrons near the chamber surface [48, 49].

- The PSR suffers from a two-stream instability caused by electrons trapped in the beam potential. Although this instability typically happens at beam currents higher than required for nominal operation, it inspired a decision to coat the chambers of the SNS with TiN [35].

- At RHIC, the above-mentioned fast vacuum pressure rise instability at high current was also controlled via TiZrV coatings [36].

- ECEs are by now a generic concern for future machines, which invoke very intense beams (LHC and its injectors, ILC DRs, MI upgrade, ...). Various mitigation mechanisms are being actively researched to control the EC at the SPS in the context of the LHC future upgrade [69].

SIMULATION OF THE ECE

Broadly speaking, depending on the approximations implemented, EC simulation codes in use today are of three kinds:

- Build-up codes.

- Instability codes.

- Self-consistent codes.

Build-up codes make the approximation that the beam is a prescribed function of space and time, and therefore is nondynamical. The electrons, on the other hand, are fully dynamical. With this kind of code one can study the build-up and decay of the EC, its density distribution, and its time and energy scales, but not the effects of the EC on the beam[2]. These codes may include a detailed model of the electron-wall interaction, and come in 2D and 3D versions. 2D codes are well suited to study the EC in certain isolated regions of a storage ring, such as in the body of magnets, and field-free regions. 3D codes are used to study the EC

[2] Actually, these codes do allow the computation of the dipole wake induced by the EC on the beam, which in turn allows a first-order computation of the coherent tune shift of successive bunches of the beam.

in magnetic regions that are essentially 3D in nature, such as fringe fields and wigglers.

Instability codes aim at studying the effects on the beam by an initially prescribed EC. In these codes the beam particles are fully dynamical, while the dynamics of the cloud electrons is limited. For example, the electron-wall interaction may be simplified or non-existent, and/or the electron distribution may be refreshed to its initial state with the passage of successive bunches.

Self-consistent codes aim to study the dynamics of the beam and the electrons under their simultaneous, mutual, interaction. Such codes are far more computationally expensive than either of the above-mentioned "first-order" codes, and represent the ultimate logical stage of the above-mentioned simulation code efforts. Self-consistent codes are beginning to yield significant results [83].

A repository website containing code descriptions and contact persons has been developed by the CARE program [84].

A SIMPLE EFFECTIVE THEORY

By "simple effective theory" we mean an equation, or set of equations, that can be solved analytically, and whose solution might be used to interpret detailed simulation results, or measurements, in terms of a few effective parameters. An "effective parameter" is a combination of basic parameters, such as those fed to a simulation via the input file, and is usually averaged over a certain length of time and over the cloud electrons. Thus an effective theory has no genuine predictive power; however, the effective parameters extracted from fits to the data might give useful information about the basic parameters, and about the basic dynamics of the cloud. We already defined the effective SEY $\delta_{\rm eff}$; a few more effective parameters appear in the analysis below. In addition, identifying effective parameters in EC dynamics may help in defining a more useful, and much reduced, "parameter phase space" for the EC dynamics, and in extrapolating the results from one storage ring to another.[3]

As in other approaches [85], the essence of the procedure to find an effective theory is to integrate out the electron dynamics over the shortest time scales, thereby reaching a simplified equation involving the evolution of the EC density at longer time scales. In the discussion below, "short" means comparable to the bunch length, while "long" means comparable to the bunch spacing. This definition of "short," however, may be different in the case of hadron machines; in any case, "short times" really means time scales for a typical electron to move across the chamber by a reasonable fraction of the chamber radius under the influence of the bunch.

Let $N_e(t)$ be the number of cloud electrons at time t in a chamber section of length L being simulated. Assuming that there is no net flow of electrons into or out from this section, simple charge conservation implies that the time derivative of N_e is

$$\dot{N}_e = \dot{N}_{\rm prim} + \underbrace{\dot{N}_{\rm sec} - \dot{N}_{\rm col}}_{\text{net secondaries}} \tag{3}$$

where $\dot{N}_{\rm prim}$ is the rate of primary electrons generated by the beam by all mechanisms, $\dot{N}_{\rm col}$ is the rate of electron-wall collisions, and $\dot{N}_{\rm sec}$ is the rate of secondary electrons generated in such collisions. The effective SEY is given by $\delta_{\rm eff} = N_{\rm sec}/N_{\rm col} \simeq \dot{N}_{\rm sec}/\dot{N}_{\rm col}$. Dividing by L and multiplying by the electronic charge e yields

$$\dot{\lambda}_e(t) = \frac{e\dot{N}_{\rm prim}}{L} + (\delta_{\rm eff} - 1)pJ \tag{4}$$

where $\lambda_e = eN_e/L$ is the EC line density, p is the perimeter of the chamber cross section and J is the incident electron flux at the wall (with units of current per unit area).

Now $\dot{N}_{\rm prim}$ can be expressed in terms of the instantaneous beam current and primary electron generation parameters (see below). Let n'_p be the number of primary electrons generated per beam particle per unit length of beam traversal. If v_b is the speed of the beam, the number of primary electrons generated per unit time per beam particle is

$$\dot{n}_p = v_b n'_p \tag{5}$$

As for the time dependence of n'_p, the fact that the primary electron-generation processes are incoherent implies that $n'_p(t) \propto I_b(t)$ where $I_b(t)$ is the instantaneous beam current at this location [31]. Simple geometrical arguments yield

$$\frac{e\dot{N}_{\rm prim}}{L} = \dot{n}_p \lambda_b(t)/Z \tag{6}$$

where $\lambda_b(t) = I_b(t)/v_b$ is the instantaneous beam line density and Z is the beam-particle charge in units of e (i.e., $Z = 1$ for protons and positrons, $Z = 79$ for fully stripped gold ions, etc.), hence[4]

$$\dot{\lambda}_e(t) = \dot{n}_p \lambda_b(t)/Z + (\delta_{\rm eff} - 1)pJ \tag{7}$$

Using now $J = eN_e/(A\Delta t_{\rm tr}) = \lambda_e/(p\Delta t_{\rm tr})$ where A is the surface area of the chamber section being simulated and $\Delta t_{\rm tr}$ is the characteristic traversal time of the electrons across the chamber, we obtain

$$\dot{\lambda}_e(t) = \dot{n}_e \lambda_b(t)/Z + \frac{\lambda_e(t)}{\tau} \tag{8a}$$

$$\tau = \frac{\Delta t_{\rm tr}}{\delta_{\rm eff} - 1} \tag{8b}$$

At this point the careful reader is probably concerned with issues of sign. As written, Eqs. (7,8) are valid provided that the quantities e, λ_e, λ_b, Z and J are taken to be

[3] Although work began in 2005, a summary of this effective theory was first presented at the 21 October, 2009, meeting of the CesrTA collaboration.

[4] In Eq. (7) Z appears explicitly because $\dot{n}_p$ is the electron production rate *per beam particle*, not *per unit beam charge*. I am indebted to M. Blaskiewicz for bringing this equation to my attention.

positive. Note, however, that τ can be > 0 or < 0 depending upon the value of $\delta_{\rm eff}$.

We shall not consider the case in which there is a net influx or outflow of electrons through the ends of the chamber section being analyzed.

Simplest approximations.

Eqs. (7)-(8) for $\dot{\lambda}_e(t)$ are quite general, hence quite useless, unless further approximations are made. The quantities τ, $\Delta t_{\rm tr}$ and $\delta_{\rm eff}$ are all dynamical "effective" quantities; only $\lambda_b(t)$ and Z are a priori well known.

We first calculate the various contributions to $\dot{n}_p$ from other quantities. For example, the contribution from photoemission is given by

$$n'_p = Y_{\rm eff}\, n'_\gamma \tag{9}$$

where n'_γ is the number of photons striking the vacuum chamber wall that are emitted per beam particle per unit length of trajectory (which can be computed from standard synchrotron radiation formulas), and $Y_{\rm eff}$ is the effective quantum efficiency of the chamber surface. This latter must take into account factors such as the photon reflectivity of the surface, the photon angle of incidence, the photon energy spectrum, and the possible existence of an antechamber through which most photons can escape. Other contributions to $\dot{n}_p$ can be estimated via standard formulas depending on one or a few parameters [31].

The next step consists in simplifying the 2nd term in the right-hand side of Eqs. (7)-(8). We consider a beam composed of bunches spaced by a distance (in the Lab frame) $s_b = v_b t_b$, where t_b is the bunch spacing in time. Each bunch has a population N_b so that the bunch charge is $Q_b = eZN_b$. We now replace $\lambda_b(t)$ by its time average[5] $\lambda_b(t) \to \bar{\lambda}_b = Q_b/s_b$. Using $\dot{n}_p/s_b = n'_p/t_b$ one obtains the first-order differential equation

$$\dot{\lambda}_e(t) = \frac{\lambda_p}{t_b} + \frac{\lambda_e(t)}{\tau} \tag{10}$$

where $\lambda_p \equiv eN_b n'_p$ is the primary-electron line density.

Finally, we make the additional approximation, arrived at with a great deal of hindsight and experience from simulations, that $\delta_{\rm eff}$ and $\Delta t_{\rm tr}$, and hence τ, are constant during a meaningful length of time, i.e., at least several bunch passages. Eq. (10) can then be readily integrated. If the beam is injected into an empty chamber, i.e. no pre-existing ecloud, at $t = 0$, one obtains the build-up expression

$$\lambda_e(t) = \lambda_p(\tau/t_b)(e^{t/\tau} - 1) \tag{11}$$

For short times, $|t/\tau| \ll 1$, one finds the linear behavior

$$\lambda_e(t) \simeq \frac{\lambda_p t}{t_b} \tag{12}$$

independent of τ (and therefore of $\delta_{\rm eff}$ and $\Delta t_{\rm tr}$). This behavior shows that the initial build-up of the ecloud is dominated by primary electrons, as it should be expected.

When $\delta_{\rm eff} < 1$ (i.e., $\tau < 0$) the chamber walls act as net absorbers of electrons hence $\lambda_e(t)$ reaches saturation after a time interval long enough that the number of primary electrons generated per unit time equals the number of electrons absorbed by the walls per unit time. The saturated value can be obtained by setting $\dot{\lambda}_e = 0$ in Eq. (10) or by taking the $t \to \infty$ limit of Eq. (11),

$$\lambda_{\rm sat} = -\lambda_p \tau/t_b \qquad (\tau < 0) \tag{13a}$$

$$= \frac{\lambda_p \Delta t_{\rm tr}}{t_b(1-\delta_{\rm eff})} \qquad (\delta_{\rm eff} < 1) \tag{13b}$$

A rough estimate of $\Delta t_{\rm tr}$ can be obtained by computing the traversal time along a chamber diagonal of an electron born at rest at a point in the chamber under the action of a single ultrarelativistic bunch in the impulse approximation, neglecting space-charge and image forces. Under these assumptions, a straightforward calculation yields [63]

$$\Delta t_{\rm tr} = \frac{b^2}{ZN_b r_e c} \tag{14}$$

where r_e is the classical radius of the electron (this expression assumes a round chamber of radius b; if it's not round, then b represents the smallest of the half-height or half-width), therefore[6]

$$\lambda_{\rm sat} = \frac{en'_p b^2}{(1-\delta_{\rm eff})Z s_b r_e} \qquad (\delta_{\rm eff} < 1) \tag{15}$$

This expression agrees well with simulations for the case of short bunches, provided $\delta_{\rm eff}$ is < 1 but not too close to 1. Of course, in this situation, the ECE is typically a weak effect, hence not of much practical importance.

If the beam is extracted from the chamber at $t = t_0$, the solution of Eq. (10) is

$$\lambda_e(t) = \lambda_e(t_0) e^{(t-t_0)/\tau} \tag{16}$$

In this case, expression (14) for $\Delta t_{\rm tr}$ cannot be correct because there is no beam present. One might attempt to express $\Delta t_{\rm tr}$ in terms of the residual electron cloud kinetic energy $E = kT$, where T is the EC effective temperature and k Boltzmann's constant,

$$\Delta t_{\rm tr} = \frac{b}{c}\sqrt{\frac{2mc^2}{kT}} \tag{17}$$

where m is the mass of the electron, hence

$$\tau = \frac{(b/c)}{\delta_{\rm eff} - 1}\sqrt{\frac{2mc^2}{kT}} \tag{18}$$

We shall not address the case of EC decay any further, because simulation experience shows that there does not

[5] This simplification is not essential; see the section on space-charge effects below.

[6] $\Delta t_{\rm tr}$ and t_b are related by the the Gröbner parameter $G \equiv t_b/\Delta t_{\rm tr} = N_b s_b r_e/b^2$.

seem to be any regime in which τ given by Eq. (18) is constant for a meaningful length of time—the observed decay is not quite exponential. Although the agreement with simulations is qualitatively reasonable, more research is needed.

If $\delta_{\rm eff} > 1$ then $\tau > 0$ and Eq. (11) implies that the ecloud density grows exponentially without bound, as long as there is beam present. This unphysical behavior is a consequence of our assumption that space-charge forces are negligible, which becomes invalid when the EC density is high enough. In effect, τ cannot be a constant > 1 forever—see the section below on space-charge effects.

Solution for a bunched beam.

Assuming that the bunch length is short enough that its force on the electrons is sensibly impulsive, and assuming that one injects a bunch train into an empty chamber at $t = 0$, then

$$\lambda_b(t) = \frac{Q_b}{v_b} \sum_{k=0}^{\infty} \delta(t - kt_b) \tag{19}$$

Plugging (19) into (7) one gets

$$\dot{\lambda}_e(t) = \lambda_p \sum_{k=0}^{\infty} \delta(t - kt_b) + \frac{\lambda_e(t)}{\tau} \tag{20}$$

whose solution is the stepwise function

$$\lambda_e(t) = \lambda_p \sum_{k=0}^{[t/t_b]} e^{kt_b/\tau} \tag{21}$$

where $[t/t_b]$ represents the largest integer $\leq t/t_b$. For $t/t_b \gg 1$ this yields

$$\begin{aligned} \lambda_e(t) &\simeq \lambda_p \int_0^{t/t_b} dk\, e^{kt_b/\tau} \\ &= \lambda_p(\tau/t_b)(e^{t/\tau} - 1) \end{aligned} \tag{22}$$

which is identical to (11). Therefore, within the stated approximations in this model, a continuous beam yields the same results, in the long term, as a bunched beam.

Space-charge effects.

When the SEY is large enough, $\delta_{\rm eff}$ exceeds 1 hence Eq. (8b) implies $\tau > 0$, hence the solution of Eq. (10) grows exponentially forever. This unphysical situation is controlled, in reality, by the space-charge forces which push the electrons back into the walls when λ_e becomes large enough. All simulations for which $\delta_{\rm eff} > 1$ show linear growth of $\lambda_e(t)$ when t is small enough that the process is dominated by primaries, followed by exponential growth when the process is dominated by secondaries if $\delta_{\rm eff} > 1$, followed, in turn, by saturation as $\delta_{\rm eff}$ decreases towards 1 from above as the space-charge forces make the rate of secondary electron absorption equal to the rate of secondary electron creation. A plausible and simple way to describe this effect is to make the assumption

$$\delta_{\rm eff} - 1 = \kappa \left(\frac{\lambda_c - \lambda_e}{\bar{\lambda}_b} \right) \tag{23}$$

where the constants κ and λ_c remain to be expressed in terms of more fundamental quantities, and $\bar{\lambda}_b$ is included as a convenient normalization. Eq. (23) expresses the simple fact that the above-mentioned approach $\delta_{\rm eff} \to 1$ is in simple proportion to the difference of the average EC density n_e relative to some critical value $n_c \equiv \lambda_c/(eS)$, where S is the area of the chamber cross section. With assumption (23), Eq. (7) becomes

$$\dot{\lambda}_e = \dot{n}_p \lambda_b / Z + \kappa(\lambda_c - \lambda_e) \frac{\lambda_e(t)}{\bar{\lambda}_b \Delta t_{\rm tr}} \tag{24}$$

Replacing $\lambda_b \to \bar{\lambda}_b$ and defining the scaled variables $x = t/t_b$ and $y = \lambda_e/\bar{\lambda}_b$ we obtain the first-order nonlinear equation

$$\frac{dy}{dx} = \alpha + \beta(y_c - y)y \tag{25}$$

where

$$y_c = \lambda_c/\bar{\lambda}_b \tag{26a}$$

$$\alpha = \dot{n}_p t_b / Z = n'_p s_b / Z \tag{26b}$$

$$\beta = \kappa t_b / \Delta t_{\rm tr} \tag{26c}$$

whose solution, assuming $y(0) = 0$, is readily found to be

$$y(x) = \frac{-y_+ y_- (g(x) - 1)}{y_+ - y_- g(x)} \tag{27}$$

where

$$g(x) \equiv e^{\beta(y_+ - y_-)x} \tag{28}$$

and where $y_\pm$ are the roots of the quadratic equation $\alpha + \beta(y_c - y)y = 0$, given by

$$y_\pm = \tfrac{1}{2}(y_c \pm \sqrt{y_c^2 + 4\alpha/\beta}) \tag{29}$$

Note that the exponential growth rate constant τ is given by

$$\frac{t_b}{\tau} = \beta \sqrt{y_c^2 + 4\alpha/\beta} \tag{30}$$

and the saturation level by

$$y_{\rm sat} = \lim_{x \to \infty} y(x) = y_+ \tag{31}$$

Eq. (27) has the desired features exhibited by space-charge-limited simulations, namely the behavior of $y(x)$ is linear at small x (and in agreement with Eq. (12)), exponential at intermediate x, and saturates at large x, provided the parameters are in the appropriate regime. In practical applications (see below), α is $\mathcal{O}(10^{-2})$ while β and y_c are $\mathcal{O}(0.1 - 10)$, so that $y_{\rm sat} \gtrsim y_c$. The excess $y_{\rm sat} - y_c$ is due to the contribution from the primary electrons, proportional to α.

In addition, Eq. (27) has the desired features when space-charge forces are not important, represented by Eq. (11). In this case, choosing $\kappa < 0$ (hence $\beta < 0$) ensures that $\delta_{\rm eff}$ remains < 1. In this case, the saturated level is $y_{\rm sat} \simeq -\alpha/(\beta y_c)$. Comparing Eqs. (10)-(24), and neglecting λ_e relative to λ_c, one obtains

$$\frac{t_b}{\tau} = \beta y_c \tag{32}$$

As mentioned above, this effective theory invokes two new parameters: κ describes, effectively, the growth rate of the EC while y_c determines its saturation level. The expectation that the space-charge-dominated EC level saturates when $\lambda_e \simeq \bar{\lambda}_b$ implies[7] $y_c \simeq 1$. Within the described model, however, κ and y_c are free, therefore more research is needed to interpret these parameters, and hence to fix them, in terms of other physical variables.

Tests of the effective theory

As mentioned above, the effective theory has no genuine predictive power. Nevertheless, one can test it against measurements or simulations. The test consists of two steps:

1. Does the functional dependence of Eqs. (11) or (27) fit the data?

2. If so, are the parameters extracted from the fit, such as $\delta_{\rm eff}$, τ, $\lambda_{\rm sat}$ etc., reasonable and/or consistent with the data?

We now carry out such a test for the simplest case, namely for a round beam traversing a field-free region in a round chamber in which photoelectrons are uniformly generated around the perimeter of the chamber cross section. The exercise is carried out by fitting the effective theory against simulations obtained with the code POSINST [68, 86–88]. Beam and ring parameters correspond to a section of the CesrTA storage ring, except that we assume the beam to be round instead of flat. Detailed values are listed in Table 1. Note that these parameters imply

$$\bar{\lambda}_b = \frac{eZN_b}{s_b} = 2.67 \times 10^{-9}\ {\rm C/m} \tag{33a}$$

$$\lambda_p = eN_b n'_p = 2.80 \times 10^{-11}\ {\rm C/m} \tag{33b}$$

In order to isolate the effects of space-charge, we actually carry out two tests corresponding to two values for the peak SEY. The low value, $\delta_{\rm max} = 0.8$, leads to a low EC density, hence to correspondingly weak space-charge forces. In this case we switch off the computation of space-charge in POSINST. The higher value, $\delta_{\rm max} = 2.0$, leads to a space-charge dominated EC density; in this case we use a 64×64 space-charge grid. Although these two choices for $\delta_{\rm max}$ are within a reasonable range for actual surfaces, they do not necessarily correspond to any given material. Rather, these values are meant to define two distinct regimes in the analysis of the effective theory.

[7] The value $\lambda_{\rm sat}/\bar{\lambda}_b \simeq 1$, however, is generally only in qualitative agreement with our simulations, which typically yield $\lambda_{\rm sat}/\bar{\lambda}_b \simeq 0.5-4$.

Table 1: Input Simulation Parameters.

Ring and beam	
Ring circumference	$C = 768.43$ m
Beam energy	$E = 5.3$ GeV
Revolution period	$T_0 = 2.563\ \mu$s
RF frequency	$f_{\rm RF} = 499.76$ MHz
Harmonic number	$h = 1281$
Bunch profile	3D gaussian
RMS bunch length	$\sigma_z = 1$ cm
Trans. RMS bunch sizes	$(\sigma_x, \sigma_y) = (1, 1)$ mm
Bunch population	$N_b = 7 \times 10^{10}$
Bunch spacing	7 buckets
	($t_b = 14.01$ ns, $s_b = 4.2$ m)
No. of bunches in train	45
Total no. of buckets	500 (=1 μs)
Vacuum chamber	round, radius$= 4.45$ cm
Section type	field-free region
Primary e$^-$ sources	
Photon reflectivity	$R_\gamma = 1$ (uniform illumination)
Photon generation rate	$n'_\gamma = 2.5 \times 10^{-2}$ (γ/e$^+$)/m
Quantum efficiency	$Y_{\rm eff} = 0.1$
Photoel. generation rate	$n'_p = 2.5 \times 10^{-3}$ (e$^-$/e$^+$)/m
Secondary e$^-$ parameters	
Peak SEY	$\delta_{\rm max} = 0.8$ or 2.0
Energy at $\delta_{\rm max}$	$E_{\rm max} = 292.6$ eV
SEY at 0 energy	$\delta(0) = 0.2438 \times \delta_{\rm max}$
Simulation parameters	
Primary macroelectrons/bunch	1000
Max. no. of macroelectrons	20000
Full bunch length	$L_b = 5\sigma_z$
Integration time step	4.17×10^{-11} s
Space-charge grid (if used)	64×64

For the case with $\delta_{\rm max} = 0.8$ the results are shown in Fig. 2. The red dashed line is the one-parameter fit of Eq. (11) to the simulation, which yields $\tau = -77.9$ ns. Inserting this value into Eq. (13a) yields $\lambda_{\rm sat} = 1.56 \times 10^{-10}$ C/m. Note that this value of $\lambda_{\rm sat}$ implies an average neutralization level

$$\frac{\lambda_{\rm sat}}{\bar{\lambda}_b} = 0.058 \tag{34}$$

which is sufficiently low to sensibly justify the absence of space-charge forces.

It is clear that the functional form of the fit in Fig. 2 is a very good description of the simulation data. But is the extracted value of $\delta_{\rm eff}$ consistent with the other results of the simulation? This can be judged by the results in Fig. 3, which shows the simulated average SEY as a function of

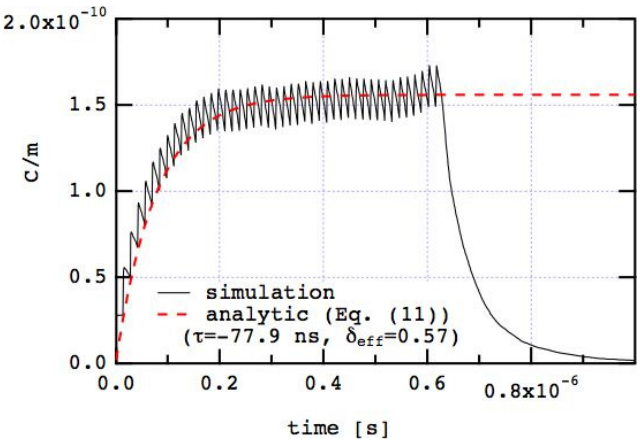

Figure 2: Average EC line density when $\delta_{\max} = 0.8$ (negligible space-charge). The red dashed line is Eq. (11) for the indicated parameter values. The end of the 45-bunch train occurs at $t \simeq 0.62$ μs.

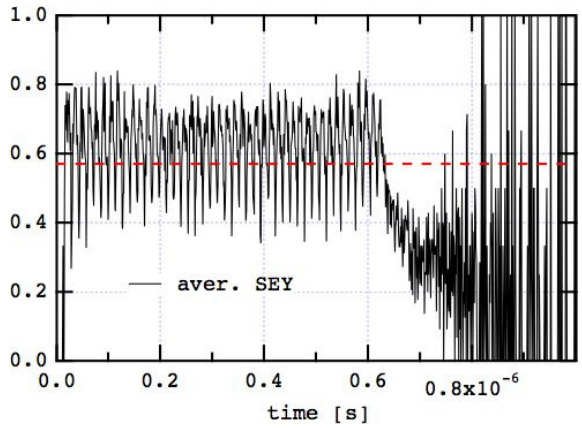

Figure 3: Simulation results for the SEY as a function of time. Plotted is the SEY averaged over all electron-wall collisions during successive time intervals of duration 1 ns. The red dashed line corresponds to $\delta_{\text{eff}} = 0.57$, the value extracted from the analytic fit.

time. It is clear that, as long as the beam is present, the average SEY is $\lesssim 0.6$, in good agreement with $\delta_{\text{eff}} = 0.57$, the value extracted from the above fit using Eq. (15). This provides further justification of the goodness of the effective theory, at least in this case.

We now address the space-charge-dominated case, corresponding to the choice $\delta_{\max} = 2.0$. In this case, the input parameters in Table 1 inserted into Eq. (26b) yield

$$\alpha = n_p' s_b = 0.0105 \tag{35}$$

Results are shown in Fig. 4. In this case, the analytic fit with Eq. (27) involves two fitting parameters, namely β and y_c, whose values are given in the figure. In this case, the large value for $\lambda_{\text{sat}}/\bar{\lambda}_b \simeq \lambda_c/\bar{\lambda}_b = 4.43$ implies an overneutralized beam (on average), confirming the dominance of space-charge forces.

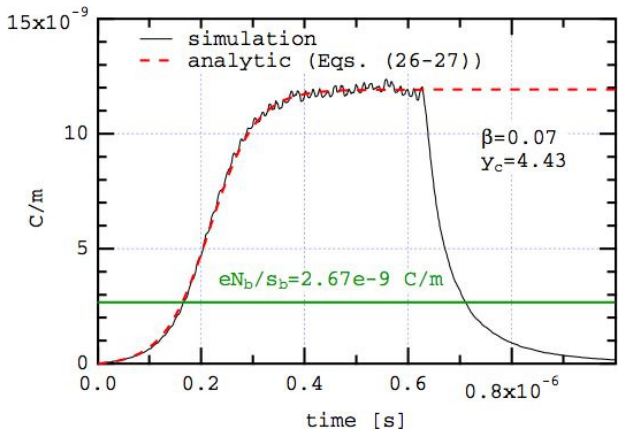

Figure 4: Average EC line density when $\delta_{\max} = 2.0$ (space-charge dominated case). The red dashed line is Eq. (27) when the fitting parameters β and y_c (Eq. (26)) take on the indicated values. The green line represents $\bar{\lambda}_b$, Eq. (33a).

While the functional form of the fit in Fig. 4 is rather exquisite, another quantitative measure of the goodness of the space-charge-dominated effective theory can be ascertained by examining how well is Eq. (23) satisfied by the simulation. First, we determine the value of κ from Eq. (26c),

$$\kappa = \beta \frac{\Delta t_{\text{tr}}}{t_b} = 0.167 \tag{36}$$

where we used $\beta = 0.07$ and we assumed the validity of the impulse approximation for Δt_{tr}, Eq. (14). We then rewrite Eq. (23) in the form

$$\delta_{\text{eff}} - 1 = \kappa \left(y_c - \frac{\lambda_e}{\bar{\lambda}_b} \right) \tag{37}$$

and insert into (37) the above-mentioned values for y_c, κ and $\bar{\lambda}_b$ plus the simulation results for δ_{eff} and λ_e. The comparison of the resulting left-hand and right-hand sides of this equation is shown in Fig. 5. We see here that the agreement of both sides of Eq. (37) is only qualitative. Unfortunately, in this comparison there is a significant confounding factor, namely that Δt_{tr} is computed in the impulse approximation neglecting space-charge and image forces, hence this test is not expected to be quantitatively accurate. Indeed, the value we used to obtain κ, $\Delta t_{\text{tr}} = 33.5$ ns obtained from Eq. (14), is more than double the bunch spacing, hence this value of Δt_{tr} probably does not represent well the time scale of the dynamics of a typical electron. For this reason, we are puzzled by the fact that the above value for Δt_{tr} seems to give much better results for the non-space-charge-dominated case than for the space-charge-dominated case. More research is needed; in any case, we take a fair amount of comfort in the qualitative agreement shown in Fig. 5.

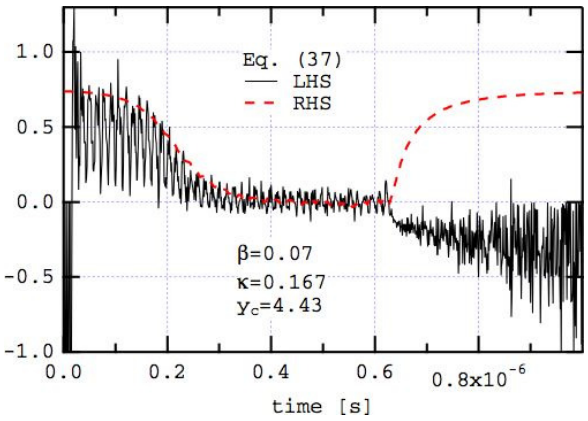

Figure 5: Left-hand side and right-hand side of Eq. (37) for the indicated values of y_c, β and κ.

Limitations

The unexpectedly good agreement between the effective theory and simulation for the space-charge-dominated case presumably implies that Eq. (23) has a more fundamental validity than a simple *ansatz*—theoretical research along these lines seems worth pursuing. Tests of the effective theory carried out in a region with a dipole magnetic field show quantitative agreement with simulations only within factors of ~ 2, although the general qualitative trends are correct. Presumably, this is because the magnetic field spoils the cylindrical symmetry of the system that is in effect in the field-free example presented above. We have not attempted to test the effective theory in a non-cylindrical chamber.

It is easy to augment, or complicate, the above effective theory in order to make it better agree with data, via the introduction of new parameters. For example, a simple extension of the basic assumption expressed by Eq. (23), which seems to be suggested by simulation results in some cases, might be given by

$$\delta_{\rm eff} - 1 = \kappa \left(\frac{\lambda_c - \lambda_e}{\bar{\lambda}_b} \right)^q \qquad (38)$$

where q is another fitting parameter. It seems to us that such improvements will not lead to an increase in the basic understanding of the dynamics. A better approach would be to inject more physical modeling into the ingredients of effective theory, thereby providing meaning to the newly introduced effective parameters. In this way, a fit to the data would provide meaningful insights.

However, even qualitative agreement between the effective theory and data (simulated or real) helps to identify and evaluate effective parameters, and this is perhaps the most significant value of such theories.

CONCLUSIONS

Understanding of the dynamics of the EC has progressed much since the mid-90's, when the effect was identified at the KEK PF. Interest in the ECE has remained persistently high ever since, in both realms of positron and proton (or ion) machines. It is perhaps fair to say that the fundamental reason for the complexities of the dynamics, and the steady stream of surprises that the EC has revealed over the years, is due to the broad range of time scales involved in the dynamics. This broad range, in turn, can be attributed to the large difference in the EC energy scales, typically tens of eV's, and the typical beam energy scales, typically GeV's. In addition, given that the dynamics mixes details of the beam with geometric and electronic properties of the vacuum chamber surface, there is a large number of variables involved, whose relative relevance generally changes from one machine to another.

Nevertheless, though much progress has been made, including the benchmarking and validation of simulation codes, and the identification of several relevant variables, we do not yet have reliable, simple, rules of thumb to decide a priori (i.e., without extensive simulations) when any given machine will be "safe" vis-à-vis the ECE. We can reasonably forecast when the effect will be severe, but not very well when the effect will be weak. For example, we would like to develop criteria akin to current thresholds for instabilities triggered by conventional impedances. Effective theories may help to simplify the picture, and hopefully to better allow extrapolations from one case to another.

Finally, with its comprehensive combination of measurements, simulations, diagnostics and analysis, CesrTA is without a doubt the most significant, dedicated, systematic program devoted to understand the ECE not only in e^+e^- rings, but its generic aspects as well, which are already benefitting hadron machines such as the LHC. Although funding started only $\sim$3 years ago, progress has been truly major. This ECLOUD10 workshop is rightfully sited at Cornell.

ACKNOWLEDGMENTS

Over the years I have greatly benefitted from discussions and/or collaboration with many colleagues at ANL, BNL, CERN, Cornell, FNAL, Frascati, KEK, LANL, LBNL, SLAC and TechX—I am grateful to all of them. I want to express my special thanks to Mark Palmer for organizing this productive and enlightening workshop.

REFERENCES

[1] Proc. Intl. Workshop on Collective Effects and Impedance for B Factories "CEIBA95" (KEK, Tsukuba, Japan, 12-17 June 1995; Y. H. Chin, ed.), KEK Proceedings 96-6, August 1996.

[2] Workshop on Electron Effects in High-Current Proton Rings (SNS/LANL, Santa Fe, NM, 4-7 March 1997), LA-UR-98-1601.

[3] Proc. Intl. Workshop on Multibunch Instabilities in Future Electron and Positron Accelerators "MBI97" (KEK, Tsukuba, Japan, 15-18 July 1997; Y. H. Chin, ed.),

KEK Proceedings 97-17, December 1997, http://www-acc.kek.jp/WWW-ACC-exp/Conferences/MBI97-N/MBI97.html

[4] Proc. Workshop in Instabilities of High Intensity Hadron Beams in Rings "HB1999" (BNL, Upton, NY, June. 28 - July 1, 1999; T. Roser and S.Y. Zhang, eds.), AIP Conf. Proc. 496.

[5] Proc. 8th Advanced Beam Dynamics ICFA Mini-Workshop on Two-Stream Instabilities in Particle Accelerators and Storage Rings "TwoStream2000" (Santa Fe, NM, 16–18 Feb. 2000; K. Harkay and R. Macek, eds.), http://www.aps.anl.gov//News/Conferences/2000/icfa/two-stream.html

[6] Intl. Workshop on Two-Stream Instabilities in Particle Accelerators and Storage Rings "TwoStream2001" (KEK, Tsukuba, Japan, Sept 11–14, 2001), http://conference.kek.jp/two-stream/.

[7] Proc. 20th ICFA Advanced Beam Dynamics Workshop on High Intensity High Brightness Hadron Beams "HB2002" (FNAL, April 8–12, 2002; W. Chou and Y. Mori, eds.), http://proceedings.aip.org/proceedings/confproceed/642.jsp

[8] Proc. Mini-Workshop on Electron-Cloud Simulations for Proton and Positron Beams "ECLOUD02" (CERN, Apr. 15-18, 2002; F. Zimmermann and G. Rumolo, eds.), CERN Yellow Report CERN-2002-001 (2002), http://slap.cern.ch/collective/ecloud02/

[9] Mini-Workshop on SPS Scrubbing Run Results and Implications for the LHC (CERN, 28 Jun. 2002), http://sl.web.cern.ch/SL/sli/scrubbing-2002/workshop.htm

[10] 13th ICFA Beam Dynamics Mini-Workshop on Beam-Induced Pressure Rise in Rings "Prise2003" (BNL, Dec. 9-12, 2003), http://www.c-ad.bnl.gov/icfa/

[11] Proc. 31st ICFA Advanced Beam Dynamics Workshop on Electron-Cloud Effects "ECLOUD04" (Napa, California, April 19-23, 2004; M. Furman, S. Henderson and F. Zimmermann, eds.), CERN Yellow Report CERN-2005-001/CARE-Conf-05-001-HHH/LBNL-56372/SNS-10400000-TR0024-R00, http://icfa-ecloud04.web.cern.ch/icfa-ecloud04/

[12] Proc. 33rd ICFA Advanced Beam Dynamics Workshop on High Intensity and High Brightness Hadron Beams "HB2004" (Bensheim, Germany, Oct. 18-22, 2004; I. Hofmann and J.-M. Lagniel, eds.). AIP Conf. Proc. 773, BNL-73262-2004-AB (2004), http://www.gsi.de/search/events/conferences/ICFA-HB2004/index_e.html

[13] Proc. 1st CARE-HHH-APD Workshop on Beam Dynamics in Future Hadron Colliders and Rapidly Cycling High-Intensity Synchrotrons "HHH2004" (CERN, 8–11 November 2004; F. Ruggiero and F. Zimmermann, eds.), http://care-hhh.web.cern.ch/care-hhh/HHH-2004/

[14] 39th ICFA Advanced Beam Dynamics Workshop on High Intensity High Brightness Hadron Beams "HB2006" (Epochal Intl. Congress Center, Tsukuba, Japan, May 29 - June 2, 2006), http://hb2006.kek.jp/. Proceedings: http://accelconf.web.cern.ch/accelconf/abdwhb06/indexloc.htm

[15] Joint CARE-HHH, CARE-ELAN and EuroTeV Mini-Workshop on Electron-Cloud Clearing "ECL2" (CERN, 1-2 Mar. 2007), http://care-hhh.web.cern.ch/care-hhh/ECL2/

[16] Proc. Intl. Workshop on Electron-Cloud Effects "ECLOUD07" (Daegu, S. Korea, April 9-12, 2007; H. Fukuma, E. S. Kim and K. Ohmi, eds.), KEK Proceedings 2007-10, Dec. 2007, http://chep.knu.ac.kr/ecloud07/

[17] 42nd ICFA Advanced Beam Dynamics Workshop on High-Intensity, High-Brightness Hadron Beams "HB2008" (Nashville, TN, Aug. 25-29, 2008), http://neutrons.ornl.gov/workshops/hb2008/

[18] CARE-HHH-APD Mini-Workshop on Electron-Cloud Mitigation "ECM08" (CERN, 20-21 Nov. 2008), http://indico.cern.ch/conferenceDisplay.py?confId=42645

[19] EuCARD-AccNet-EuroLumi Workshop on Anti E-Cloud Coatings That Require no Activation "AEC09" (CERN, 12-13 Oct. 2009), http://indico.cern.ch/conferenceDisplay.py?confId=62873

[20] 46th ICFA Advanced Beam Dynamics Workshop on High-Intensity and High-Brightness Hadron Beams "HB2010" (Morschach, Switzerland, Sep. 27–Oct. 1, 2010), http://hb2010.web.psi.ch/

[21] 49th ICFA Advanced Beam Dynamics Workshop on Electron Cloud Physics "ECLOUD10" (Cornell University, Ithaca, NY, USA, Oct. 8-12, 2010), http://www.lepp.cornell.edu/Events/ECLOUD10/WebHome.html

[22] EuCARD-AccNet CERN-GSI Mini Workshop on Modeling Electron-Cloud Effects (CERN, Geneva, 7-8 Mar. 2011), http://indico.cern.ch/conferenceDisplay.py?ovw=True&confId=125315

[23] Joint Accelerator Conferences Website, http://www.jacow.org/

[24] The Newsletters can be accessed from the ICFA Beam Dynamics Panel website, http://www-bd.fnal.gov/icfabd/

[25] Electron Cloud in the LHC, http://ab-abp-rlc.web.cern.ch/ab-abp-rlc-ecloud/

[26] R. Macek, A. A. Browman, J. S. Kolski, R. C. McCrady, L. J. Rybarcyk, T. Spickermann, and T. J. Zaugg, "Electron cloud generation, trapping and ejection from quadrupoles at the Los Alamos PSR," Proc. "ECLOUD10" (Ref. 21).

[27] G. Rumolo, F. Ruggiero, and F. Zimmermann, "Simulation of the Electron-Cloud Build Up and its Consequences on Heat Load, Beam Stability, and Diagnostics," PRST-AB **4**, 012801 (2001). Erratum: **4**, 029901 (2001).

[28] G. Rumolo, G. Arduini, E. Métral, E. Shaposhnikova, E. Benedetto, R. Calaga, G. Papotti, and B. Salvant, "Dependence of the Electron-Cloud Instability on the Beam Energy," Phys. Rev. Lett. **100**, 144801 (2008).

[29] M. A. Furman, "Studies of e-cloud build up for the FNAL main injector and for the LHC," Proc. "HB2006" (Ref. 14), paper TUAX05.

[30] R. Cimino, I. R. Collins, M. A. Furman, M. Pivi, F. Ruggiero, G. Rumolo, and F. Zimmermann, "Can Low Energy Electrons Affect High Energy Physics Accelerators?," CERN-AB-2004-012 (ABP), LBNL-54594, SLAC-PUB-10350, February 9, 2004; Phys. Rev. Lett. **93**, 014801 (2004).

[31] M. A. Furman, "Formation and Dissipation of the Electron Cloud," LBNL-51829; Proc. PAC03, paper TOPC001.

[32] F. Zimmermann, "Electron-Cloud Effects in the LHC," Proc. "ECLOUD02" (Ref. 8), p. 47.

[33] G. Arduini, V. Baglin, T. Bohl, B. Jenninger, M. Jiménez, J.-M. Laurent, D. Schulte, F. Ruggiero, F. Zimmermann, "Electron-cloud build-up simulations and experiments at CERN," CERN-AB-2004-082, Jul 2004; published: Proc. EPAC04, paper WEPLT044.

[34] K. Kennedy, B. Harteneck, G. Millos, M. Benapfl, F. King and R. Kirby, "TiN Coating of the PEP-II Low-Energy Ring Aluminum Arc Vacuum Chambers," Proc. PAC97, paper 8C009 (p. 3568).

[35] P. He, H.C. Hseuh, M. Mapes, R. Todd and D. Weiss, "Development of Titanium Nitride Coating For SNS Ring Vacuum Chambers," Proc. PAC01, paper WPAH034 (p. 2159).

[36] W. Fischer, M. Blaskiewicz, J. M. Brennan, H. Huang, H. C. Hseuh, V. Ptitsyn, T. Roser, P. Thieberger, D. Trbojevic, J. Wei, S. Y. Zhang, and U. Iriso, "Electron cloud observations and cures in the Relativistic Heavy Ion Collider," PRST-AB **11**, 041002 (2008).

[37] H. C. Hseuh, M. Mapes, L. A. Smart, R. Todd and D. Weiss, "Upgrade of RHIC Vacuum Systems for High Luminosity Operation," Proc. PAC05, paper RPPE047.

[38] Y. Suetsugu, K. Kanazawa, K. Shibata, H. Hisamatsu, K. Oide, F. Takasaki, R. V. Dostovalov, A. A. Krasnov, K. V. Zolotarev, E. S. Konstantinov, V. A. Chernov, A. E. Bondar, A. N. Shmakov, "First experimental and simulation study on the secondary electron and photoelectron yield of NEG materials (Ti-Zr-V) coating under intense photon irradiation," NIMPR A **554** (2005) 92-113.

[39] Y. Suetsugu , K. Kanazawa, K. Shibata, H. Hisamatsu, "Continuing study on the photoelectron and secondary electron yield of TiN coating and NEG (Ti-Zr-V) coating under intense photon irradiation at the KEKB positron ring," NIMPR A **556** (2006) 399-409.

[40] Y. Suetsugu, K. Kanazawa, K. Shibata and H. Hisamatsu, "Continued Study on Photoelectron and Secondary Electron Yields of TiN and NEG (Ti-Zr-V) Coatings at the KEKB Positron Ring," Proc. PAC07, paper FRPMN042.

[41] Y. Suetsugu, K.-I. Kanazawa, K. Shibata, H. Hisamatsu, M. Shirai, "Vacuum System for High-Current e-/e+ Accelerators," ICFA Beam Dynamics Newsletter No. 48, p. 118 (April 2009).

[42] LHC Design Report, CERN-2004-003, Vol. 1, p. 346

[43] E. N. Shaposhnikova, G. Arduini, J. Axensalva, E. Benedetto, S. Calatroni, P. Chiggiato, K. Cornelis, P. Costa Pinto, B. Henrist, J. M. Jiménez, E. Mahner, G. Rumolo, M. Taborelli, C. Yin Vallgren, "Experimental Studies of Carbon Coatings as Possible Means of Suppressing Beam Induced Electron Multipacting in the CERN SPS," Proc. PAC09, paper MO6RFP008.

[44] C. Yin Vallgren, G. Arduini, J. Bauche, S. Calatroni, P. Chiggiato, K. Cornelis, P. Costa Pinto, E. Métral, G. Rumolo, E. Shaposhnikova, M. Taborelli, G. Vandoni, "Amorphus Carbon Coatings for Mitigation of Electron Cloud in the CERN SPS," Proc. IPAC10, paper TUPD048.

[45] V. Baglin, I. R. Collins, O. Gröbner, "Photoelectron Yield and Photon Reflectivity from Candidate LHC Vacuum Chamber Materials with Implications to the Vacuum Chamber Design," CERN-LHC-Project-Report-206, Jul 1998. Proc. EPAC 98, paper TUP18H.

[46] G. Stupakov and M. Pivi, "Suppression of the Effective Secondary Emission Yield for a Grooved Metal Surface," LCC-0145, SLAC-TN-04-045, June 2004; Proc. ECLOUD04 (Ref. 11), p. 139.

[47] Y. Suetsugu, H. Fukuma, K. Shibata, M. Pivi, L. Wang, "Experimental Studies On Grooved Surfaces To Suppress Secondary Electron Emission," Proc. IPAC10, paper TUPD043.

[48] A. Kulikov, A. Fisher, S. Heifets, J. Seeman, M. Sullivan, U. Wienands and W. Kozanecki, "The Electron Cloud Instability at PEP-II," Proc. PAC01, paper TPPH100 (p. 1903).

[49] Y. Funakoshi, K. Akai, A. Enomoto, J. Flanagan, H. Fukuma, K. Furukawa, J. Haba, S. Hiramatsu, K. Hosoyama, T. Ieiri, N. Iida, H. Ikeda, S. Kamada T. Kamitani, S. Kato, M. Kikuchi, E. Kikutani, H. Koiso, S. I. Kurokawa, M. Masuzawa, T. Matsumoto, T. Mimashi, T. T. Nakamura, Y. Ogawa, K. Ohmi, Y. Ohnishi, S. Ohsawa, N. Ohuchi, K. Oide, E. A. Perevedentsev, K. Satoh, M. Suetake, Y. Suetsugu, T. Suwada, F. Takasaki, M. Tawada, M. Tejima, M. Tobiyama, S. Uno, Y. Wu, N. Yamamoto, M. Yoshida, S. Yoshimoto, M. Yoshioka and F. Zimmermann, "KEKB Performance," Proc. PAC01, paper RPPH131.

[50] Y. Suetsugu, H. Fukuma, K. Shibata, M. Pivi and L. Wang, "Demonstration of Electron Clearing Effect by Means of Clearing Electrodes and Groove Structures in High-Intensity Positron Ring," Proc. PAC09, paper FR5RFP068.

[51] Y. Suetsugu, H. Fukuma, K. Shibata, M. Pivi, and L. Wang, "Beam Tests of a Clearing Electrode for Electron Cloud Mitigation at KEKB Positron Ring," Proc. IPAC10, paper WEOAMH01.

[52] F.-J. Decker, M. H. R. Donald, R. C. Field, A. Kulikov, J. Seeman, M. Sullivan, U. Wienands and W. Kozanecki, "Complicated Bunch Pattern in PEP-II," Proc. PAC01, paper TPPH126 (p. 1963).

[53] J.-L. Vay, J. M. Byrd, M. A. Furman, R. Secondo, M. Venturini, J. D. Fox, C. H. Rivetta, W. Höfle, "Simulation of E-Cloud Driven Instability and its Attenuation Using a Feedback System in the CERN SPS," Proc. IPAC10, paper WEOBRA02.

[54] J. D. Fox, A. Bullitt, T. Mastorides, G. Ndabashimiye, C. Rivetta, O. Turgut, D. Van Winkle, J. Byrd, M. Furman, J-L. Vay, W. Höfle, G. Rumolo, R. De Maria, "SPS Ecloud Instabilities - Analysis of Machine Studies and Implications for Ecloud Feedback" Proc. IPAC10, paper WEPEB052.

[55] M. Izawa, Y. Sato and T. Toyomasu, "The Vertical Instability in a Positron Bunched Beam," Phys. Rev. Lett. **74**, 5044 (1995).

[56] K. Ohmi, "Beam Photo-Electron Interactions in Positron Storage Rings," Phys. Rev. Lett. **75**, 1526 (1995).

[57] S. Heifets, "Study of an Instability of the PEP-II Positron Beam (Ohmi Effect and Multipacting)," Proc. "CEIBA95" (Ref. 1), p. 295.

[58] Z. Y. Guo, H. Huang, S. P. Li, D. K. Liu, L. Ma, Q. Qin, L. F. Wang, J. Q. Wang, S. H. Wang, C. Zhang, F. Zhou, Y.

H. Chin, H. Fukuma, S. Hiramatsu, M. Izawa, T. Kasuga, E. Kikutani, Y. Kobayashi, S. Kurokawa, K. Ohmi, Y. Sato, Y. Suetsugu, M. Tobiyama, K. Yokoya and X. L. Zhang, "The experimental study on beam-photoelectron instability in BEPC," Proc. PAC97, paper 3B012.

[59] K. C. Harkay, "Theory and Measurement of the Electron-Cloud Effect," Proc. PAC99, paper TUAL4.

[60] H. Fukuma, "Electron Cloud Instability in KEKB and SuperKEKB," ICFA Beam Dynamics Newsletter No. 48, p. 112 (April 2009).

[61] T. Holmquist and J. T. Rogers, "A Trapped Photoelectron Instability in Electron and Positron Storage Rings," Phys. Rev. Lett. **79**(17), 3186 (1997).

[62] M. A. Palmer, M. G. Billing, J. Calvey, S. S. Chapman, J. A. Crittenden, R. Gallagher, S. Gray, S. Greenwald, W. H. Hopkins, D. L. Kreinick, Y. Li, X. Liu, J. A. Livezey, R. Meller, D. P. Peterson, M. Rendina, D. Rice, N. Rider, D. Sagan, J. Sexton, J. P. Shanks, J. Sikora, S. Vishniakou, W. Whitney, T. Wilksen, H. Williams, K. C. Harkay, J. P. Alexander, G. Codner, J. Dobbins, G. Dugan, M. Forster, D. L. Hartill, V. Medjidzade, S. Peck, D. Rubin, E. Smith, K. W. Smolenski, C. R. Strohman, A. Temnykh, M. Tigner, R. Holtzapple, A. Wolski, J. Kandaswamy, Y. He, M. Ross, C.-Y. Tan, R. M. Zwaska, J. W. Flanagan, P. Jain, K.-I. Kanazawa, K. Ohmi, H. Sakai, Y. Suetsugu, J. Byrd, C. M. Celata, J. Corlett, S. De Santis, M. Furman, A. Jackson, R. Kraft, D. V. Munson, G. Penn, D. Plate, A. Rawlins, M. Venturini, M. Zisman, D. Kharakh, M. T. F. Pivi, L. Wang, J. Jones, "The Conversion and Operation of the Cornell Electron Storage Ring as a Test Accelerator (CesrTA) for Damping Rings Research and Development," Proc. PAC09, paper FR1RAI02.

[63] O. Gröbner, "Bunch-Induced Multipactoring," Proc. 10th Intl. Accel. Conf., Serpukhov, 1977, pp. 277–282.

[64] R. J. Macek, A. A. Browman, M. J. Borden, D. H. Fitzgerald, R. C. McCrady, T. Spickermann and T. J. Zaugg, "Status of Experimental Studies of Electron Cloud Effects at the Los Alamos Proton Storage Ring," Proc. "ECLOUD04" (Ref. 11), p. 93.

[65] V. Dudnikov, "Some Features of Transverse Instability of Partly Compensated Proton Beams," Proc. PAC01, paper TPPH094 (p. 1892).

[66] O. Gröbner, "Bunch-Induced Multipacting," Proc. PAC97, p. 3589.

[67] F. Zimmermann, "A Simulation Study of Electron-Cloud Instability and Beam-Induced Multipacting in the LHC," SLAC-PUB-7425, LHC Project Report 95, 27 February 1997.

[68] M. A. Furman, "The electron-cloud effect in the arcs of the LHC," LBNL-41482/CBP Note 247/CERN LHC Project Report No. 180, May 20, 1998.

[69] See, for example, the presentations by J. M. Jiménez at the Chamonix 2011 LHC Performance Workshop, 24–28 January, 2011, http://indico.cern.ch/conferenceOtherViews.py?view=standard&confId=103957

[70] G. Arduini, T. Bohl, K. Cornelis, W. Höfle, E. Métral, F. Zimmermann, "Beam Observations with Electron Cloud in the CERN PS and SPS Complex," Proc. "ECLOUD04" (Ref. 11), p. 31.

[71] K. Ohmi and F. Zimmermann, "Head-Tail Instability Caused by Electron Clouds in Positron Storage Rings," Phys. Rev. Lett. **85**(18), 3821 (2000).

[72] K. Ohmi, F. Zimmermann, E. Perevedentsev, "Wake-field and fast head - tail instability caused by an electron cloud," Phys. Rev. E**65**, 016502 (2002).

[73] F. Zimmermann, "Review of Single Bunch Instabilities Driven by an Electron Cloud," PRST-AB **7**, 124801 (2004).

[74] J. A. Crittenden, J. R. Calvey, G. F. Dugan, D. L. Kreinick, Z. Leong, J. A. Livezey, M. A. Palmer, D. L. Rubin, D. C. Sagan, K. Harkay, R. L. Holtzapple, M. A. Furman, G. Penn, M. Venturini, M. Pivi, L. Wang, "Progress in Studies of Electron-Cloud-Induced Optics Distortions at CESRTA," Proc. IPAC10, paper TUPD024.

[75] K. Ohmi and S. S. Win, "Study of Coupled Bunch Instability Caused by Electron Cloud," Proc. "ECLOUD04" (Ref. 11), p. 313.

[76] M. A. Furman and A. Zholents, "Incoherent Effects Driven by the Electron Cloud," Proc. PAC99, paper TUP130.

[77] E. Benedetto, G. Franchetti, and F. Zimmermann, "Incoherent Effects of Electron Clouds in Proton Storage Rings," Phys. Rev. Lett. **97**, 034801 (2006).

[78] G. Franchetti, I. Hofmann, W. Fischer and F. Zimmermann, "Incoherent effect of space charge and electron cloud," PRST-AB **12**, 124401 (2009).

[79] A. W. Molvik, M. Kireeff Covo, R. Cohen, A. Friedman, S. M. Lund, W. Sharp, J.-L. Vay, D. Baca, F. Bieniosek, C. Leister, and P. Seidl, "Quantitative experiments with electrons in a positively charged beam," Phys. of Plasmas **14**, 056701 (2007).

[80] T. Toyama and the e-cloud study team, KEK, "Electron Cloud Effects in the J-PARC Rings and Related Topics," Proc. "ECLOUD04" (Ref. 11), p. 77.

[81] K. G. Sonnad, C. M. Celata, M. Furman, D. Grote, J.-L. Vay, M. Venturini, "Simulations of Electron Cloud Effects on the Beam Dynamics for the FNAL Main Injector Upgrade," LBNL-63753; Proc. PAC07, paper FRPMS028.

[82] R. Zwaska, "Electron Cloud Studies in FNAL Main Injector," Proc. "HB2008" (Ref. 17).

[83] See, for example, J.-L. Vay, M. A. Furman, R. Secondo, M. Venturini, J. D. Fox, C. H. Rivetta and W. Höfle, "Direct Numerical Modeling of E-Cloud Driven Instability of a Bunch Train in the CERN SPS," Proc. "ECLOUD10" (Ref. 21).

[84] CARE HHH Electron Cloud Code Collection, https://oraweb.cern.ch/pls/hhh/code_website.disp_category?cat_name=Electron%20Cloud

[85] U. Iriso and S. Peggs, "Maps for electron clouds," PRST-AB **8**, 024403 (2005).

[86] M. A. Furman and G. R. Lambertson, "The electron-cloud instability in the arcs of the PEP-II positron ring," LBNL-41123/CBP Note-246, PEP-II AP Note AP 97.27 (Nov. 25, 1997). Proc. "MBI97" (Ref. 3), p. 170.

[87] M. A. Furman and M. T. F. Pivi, "Probabilistic model for the simulation of secondary electron emission," LBNL-49771/CBP Note-415 (Nov. 6, 2002). PRST-AB **5** 124404 (2003),

[88] M. A. Furman and M. T. F. Pivi, "Simulation of secondary electron emission based on a phenomenological probabilistic model," LBNL-52807/SLAC-PUB-9912 (June 2, 2003).